Ruthenium on beta zeolite in cinnamaldehyde hydrogenation

M. Lashdaf[a,*], M. Tiitta[b], T. Venäläinen[c], H. Österholm[b], and A.O.I. Krause[a]

[a] *Department of Chemical Technology, Helsinki University of Technology, P.O. Box 6100, FIN-02015 HUT, Finland*
[b] *Fortum Oil and Gas Oy, P.O. Box 310, FIN-06101 Porvoo, Finland*
[c] *Department of Chemistry, University of Joensuu, P.O. Box 120, FIN-08101 Joensuu, Finland*

Received 30 September 2003; accepted 2 February 2004

The behaviour of ruthenium was studied in relation to the acidity of beta zeolite. The impregnation of beta zeolite with ruthenium chloride decreased the crystallite size of beta zeolite. The acidity of the beta zeolite influenced the particle size of ruthenium. The particle size of ruthenium increased with decreasing acidity. Even catalysts with large particle size of ruthenium were selective to hydrogenation of the C=C bond in cinnamaldehyde hydrogenation. The ruthenium catalyst with highest Brönsted acidity gave the highest conversion. The products formed were hydrocinnamaldehyde, cinnamaldehyde acetal and hydrocinnamaldehyde acetal; no cinnamyl alcohol was observed, which indicates protection of the C=O group during the hydrogenation *via* acetal formation.

KEY WORDS: acidity; cinnamaldehyde; hydrogenation; ruthenium; hydrocinnamaldehyde acetal.

1. Introduction

The catalytic behaviour of ruthenium on zeolite is of interest in several different reactions, including ammonia synthesis [1], Fischer-Tropsch synthesis [2], hydrogenolysis and hydrodenitrogenation [3,4]. Recently, many studies have been focused on the catalytic activity of ruthenium zeolites in nitrogen oxide removal from exhaust gases [5–7].

Catalytic hydrogenation of unsaturated aldehydes to the unsaturated alcohols is an important reaction because of the several applications of unsaturated alcohols in the flavour and fragrance industry [8,9] and the manufacture of pharmaceuticals [10]. The cinnamaldehyde hydrogenation reaction is also of interest in many scientific investigations as a model reaction for determining the relations among catalyst activity, selectivity and catalytic properties. A comprehensive review of cinnamaldehyde hydrogenation has been presented by Gallezot *et al.* [11].

Ruthenium is one of the metals frequently used to catalyse cinnamaldehyde hydrogenation [12–14]. The behaviour of ruthenium has been studied in Y, X, L, mordenite and ZSM-5 zeolites and in mesoporous materials such as MCM-41 and MCM-48 [15–17]. There is also one study on the performance of ruthenium on beta zeolite in cinnamaldehyde hydrogenation [18]. In all these investigations, the precursor was ruthenium chloride, and it was shown that this precursor caused lower dispersion and therefore larger particle sizes relative to other precursors.

Gallezot *et al.* [11] has reported that the selectivity to cinnamyl alcohol is strongly dependent on the metal particle size of the catalysts. Galvagno *et al.* [19,20] showed that high selectivities toward cinnamyl alcohol were favoured by larger rather than smaller ruthenium particles. In contrast, in an earlier study [21] we found no cinnamyl alcohol among the products obtained with ruthenium catalysts of large particle sizes (12–13 nm). To better understand the effect of particle size, we selected a series of beta zeolites of different acidity. Zeolites are supports with well-defined acid properties [22,23] and their acidity could be expected to influence the ruthenium particle size. In this paper we report on the influence of the acidity of beta zeolites on ruthenium particle size and the consequent effects on the activity and selectivity in cinnamaldehyde hydrogenation.

2. Experimental

2.1. Preparation of the catalysts

A series of beta zeolites in proton form with different aluminium contents were purchased from TOSOH Corporation. Ruthenium on beta zeolite catalysts (Ru-Beta1, Ru-Beta2, Ru-Beta3, Ru-Beta4) were prepared by wet impregnation of $RuCl_3$ (99%, Aldrich) in a rotavapor. The ruthenium solution was prepared in a teflon-covered Berghof autoclave as follows: 4 g of $RuCl_3$ was added to 100 mL ammonia solution (25 vol%) under continuous stirring. The temperature of the autoclave was increased to 120 °C. Simultaneously, the pressure of the autoclave increased to 5 bar. The solution was kept at 120 °C for 24 h. After it reached room temperature, 300 mL of ammonia solution (25 vol%) was added. The solution was decanted and adjusted to 2000 mL. The ruthenium concentration in the solution was 560 mg/L measured by atomic absorption spectroscopy (AAS).

Zeolites were dried at 115 °C before impregnation of 6.5 g zeolite with 230 mL of the solution. The impreg-

* To whom correspondence should be addressed.

1011-372X/04/0400–0007/0 © 2004 Plenum Publishing Corporation

nation was done under vacuum at 80 °C with rotation speed of 40 rpm. The ruthenium-containing zeolite was dried at 115 °C and then calcined in a muffle oven. The heating rate was 1 °C/min to 500 °C, with hold for 2 h. The calcined materials were reduced with hydrogen in a flow reactor at 250 °C for 3 h.

2.2. Characterisation methods

Silicon and aluminium contents of beta zeolite were measured by wavelength dispersive X-ray fluorescence spectrometry (XRF, Bruker S4). The instrument is equipped with an Rh end-window X-ray tube. For the determination, a 0.5 g sample was mixed with lithium tetraborate, melted at 1350 °C and poured into a mould. The resulting glass bead is a homogeneous solid solution, which allows accurate determination of Al and Si.

The amount and type of acidity of the beta zeolites were determined by temperature programmed desorption (TPD) of ammonia and solid state proton nuclear magnetic resonance spectroscopy (^{1}H MAS-NMR). The TPD instrument was an Altamira AMI-100, equipped with a thermal conductivity detector (TCD). A 30 mg sample was mounted in a U-shaped quartz tube. In this method, the total acidity is measured by desorption of pre-adsorbed NH_3 as a function of temperature. A suitable temperature for the acidity determination, which avoided physisorbed ammonia was determined by adsorbing ammonia from 10% NH_3 in He at 100–300 °C at 50 °C intervals and then with He flushing at the same temperature. The test showed 200 °C to be suitable temperature for the adsorption. The acidity of the beta zeolite was calculated from the amount of NH_3 adsorbed at 200 °C and desorbed between 100 and 500 °C.

Since the TPD method cannot distinguish different types of acid sites, i.e. Brönsted and Lewis sites, ^{1}H MAS-NMR was used to identify the Brönsted acid sites. This method does not detect Lewis acid sites because they do not contain protons. After the sample was weighed and placed in the NMR probe, the ^{1}H MAS-NMR spectrum was recorded using a 45° excitation pulse, 64 transients, 20-s recycle time and about 10–11 kHz MAS speed. The experiment was repeated with the rotor empty and the weak signal from the empty rotor was subtracted from the signal of the sample to remove any background. A known amount of reference silica (EP10 with 19.5×10^{20} OH/g) was run under identical conditions. A quantitative determination of the H density was made by comparison of the peak areas of the reference and the sample. The assignments of the peaks were 0–1 ppm for AlOH, 1.9 ppm for SiOH and 4–7 ppm for the Al–OH–Si (H^+) Brönsted acid sites.

On the beta zeolite external acidity was determined by the adsorption of triphenylphosphine (TPP). TPP is too large to fit in the pores of beta zeolite and remains on the surface [24]. The procedure was as follows: 0.24 g of TPP was dissolved in 5 mL toluene, 2 g of dried beta zeolite was added and the mixture was stirred for 1 h at room temperature. The solution was then filtered and the solid that was filtered out was washed four times with 5 mL toluene and dried at 150 °C in an oven for 12 h. A blank test was made without TRP. The phosphorus contents of the samples were determined in helium atmosphere by a pre-calibrated XRF method. The amount of adsorbed TPP was calculated from the phosphorus content. P-NMR analysis (JEOL GSX 270-MHz NMR spectrometer) was carried out to confirm the bonding of phosphorus on the external acid sites of the beta zeolite.

Surface area and porosity of the catalyst materials before and after impregnation were determined by N_2-adsorption/desorption at liquid nitrogen temperature according to ASTM D4641. The instrument was an ASAP 2400 from Micromeritics. Data were evaluated by Data Master version 2 software. The mesoporous area and volume were calculated from the adsorption isotherm by Barrett–Joyner–Halenda (BJH) method, which is based on the Kelvin equation. The microporous area and microporosity were evaluated by the *t*-Plot method [25].

The crystal phases and crystallite sizes of the zeolite as well as of the catalysts after each step in the preparation (impregnation, calcination and reduction) were measured by X-ray diffraction (XRD). The XRD patterns were collected between 2° and 75° 2Θ in reflection mode with a Siemens D500 instrument equipped with a Cu-anode and a curved graphite monochromator in the reflected beam. The samples were dried in a sample holder at 110 °C for at least 2 h. The samples were covered by a half-cylindrical Mylar window to avoid absorption of moisture and prevent formation of crystalline hydrates. Crystallite sizes were evaluated from line broadening according to the Scherrer equation [26,27]:

$$\text{Crystallite size (nm)} = \lambda/\text{FWHM} * \cos\theta,$$

where $\lambda = 0.1542$ nm (CuKα), FWHM = full width at half maximum, and θ is the diffraction angle.

The amount of Ru in beta zeolite was determined by instrumental neutron activation analysis (INAA). The reduction behaviour of ruthenium was analysed by temperature programmed reduction (TPR) in hydrogen. The instrument was an Altamira AMI-100 equipped with a TC detector. The amount of sample used for the analysis was 100 mg. The TPR procedure included initial drying with 5% O_2 in helium at 240 °C with a ramp rate of 2 °C/min followed by an isothermal step at 240 °C for 30 min. The temperature was then decreased to 50 °C in 5% O_2 prior to reduction. The TPR curve was collected between 50 and 500 °C at a rate of 10 °C/min; the reduction gas was 11% H_2 in argon. The reduction steps occurring in TPR were identified by reducing the Ru-Beta4 sample at 120, 170, 360 and 550 °C. After each reduction in the TPR instrument, the sample was analysed by XRD.

The metal dispersion of the catalysts was determined by pulse CO chemisorption. The experiments were carried out using a Micromeritics TPD/TPR 2910 AutoChem' instrument. The sample (100–200 mg) was set in the quartz U-tube and reduced with H_2 stream (20 mL/min). A ramp rate of 10 °C/min was applied and the temperature was linearly raised to final temperature of 250 °C, where it was held for 120 min. The specimen was cooled to 35 °C under flowing He (99.9999%, AGA) and when the baseline was stable the experiment was started. Pulses of CO (99.997%, AGA) were repeated until the catalyst was saturated. The calculation of the dispersion based on the total amount of carbon monoxide assumed the stoichiometry CO/Ru = 1 [14].

2.3. Cinnamaldehyde hydrogenation

The pre-reduced catalysts were activated *in situ* in the batch reactor before cinnamaldehyde hydrogenation test under 10 bar hydrogen at 60 °C for 20 h. Cinnamaldehyde (99% GC purity) was from Merck and the solvent 2-propanol (>99% purity) was from Fluka and used as received. 2-Propanol was used as a solvent since alcohols are known to increase the conversions of cinnamaldehyde [28,29]. The batch reactor for the hydrogenation was a stainless steel autoclave of 100 cm^3 equipped with a hydrogen inlet, a glass funnel, a thermocouple and a magnet stirrer.

After the activation, the reactor was depressurised, and 10 g of the cinnamaldehyde and 10g of the solvent 2-propanol were loaded through the glass funnel into the reactor. The amount of the catalyst was 200 mg. The reaction was performed at 60 °C under 10 bar hydrogen pressure and at a stirring speed of 500 rpm. The duration of each test was 4 h. Every hour a sample was taken and analysed with a gas chromatograph, Varian 3400, equipped with a flame-ionisation detector. The GC column was DB-1 of 60 m length and 0.25 mm diameter.

The conversion, selectivity and turnover frequency (TOF) values were calculated with the following formula:

The reaction rate was calculated assuming a rate law of first order with respect to cinnamaldehyde [30].

3. Results and discussion

3.1. Characterisation of catalyst materials

The properties of the beta zeolites are listed in table 1. The silicon contents are about 43 wt% and the aluminium content varied between 0.2 and 2.3 wt%. Beta zeolites possess both Brönsted and Lewis acidity. The amount of Brönsted acid sites in the beta zeolites measured by ^1H MAS-NMR were between 30 and 270 μmol/g. Total acidities measured by NH_3-TPD ranged between 95 and 560 μmol NH_3/g and the external acidities were between 17 and 51 μmol TPP/g.

Table 2 shows a comparison of the N_2-adsorption and XRD data of supports and catalysts, impregnated and calcined. The beta zeolites appeared to suffer a 30–50% loss in zeolite crystallite size upon impregnation with ruthenium chloride. However, no indication of formation of distinct amorphous phases was detected by XRD. The decrease in surface area of the micropores showed some correlation with increase in ruthenium content. The amounts of ruthenium in the catalysts were between 1.6 and 2.4 wt%. No marked changes were observed in the surface areas of mesopores relative to ruthenium content. These observations suggest that the ruthenium could be blocking some micropores of the beta zeolites or that some reaction has occurred between $RuCl_3$ and the

Table 1
Properties of the beta zeolites

	Si, wt%	Al, wt%	Brönsted acidity, μmol/g	External surface acidity, μmol TPP/g	Total acidity, μmol NH_3/g
Beta1	43.4	2.3	110	28	560
Beta2	42.5	1.0	270	51	345
Beta3	43.0	0.8	130	41	245
Beta4	42.7	0.2	30	17	95

$$\text{Conversion } (\%) = \frac{100*(\text{initial cinnamaldehyde (wt\%)} - \text{cinnamaldehyde in product (wt\%)})}{(\text{initial cinnamaldehyde (wt\%)})}$$

$$\text{Selectivity}(\%) = \frac{100*\text{amount of product (wt\%)}}{\text{amount of all products (wt\%)}}$$

$$\text{TOF}_h(1/s) = \frac{\text{Initial reaction rate (mol cinnamaldehyde reacted to hydrogenated products/s)}}{\text{active site (mol surface Me}^\circ)}$$

$$\text{TOF}_a(1/s) = \frac{\text{Initial reaction rate (mol cinnamaldehyde reacted to acid-catalysed products/s))}}{\text{active site (mol TPP on external surface)}}$$

Table 2
Crystallite sizes and surface areas of catalyst materials before and after impregnation

Catalyst	Ru content, wt%	Crystallite size of zeolite at [302] reflection, nm		Surface area of micropores, m^2/g		Surface area of mesopores, m^2/g	
		Zeolite	Impreg. and calc.	Zeolite	Impreg. and calc.	Zeolite	Impr. and calc.
Ru-Beta1	2.2	22.5	16.5	520	390	85	85
Ru-Beta2	1.6	25.0		555	440	85	105
Ru-Beta3	2.4	21.5	16.5	535	340	95	105
Ru-Beta4	2.3	22.5	10.0	510	355	95	80

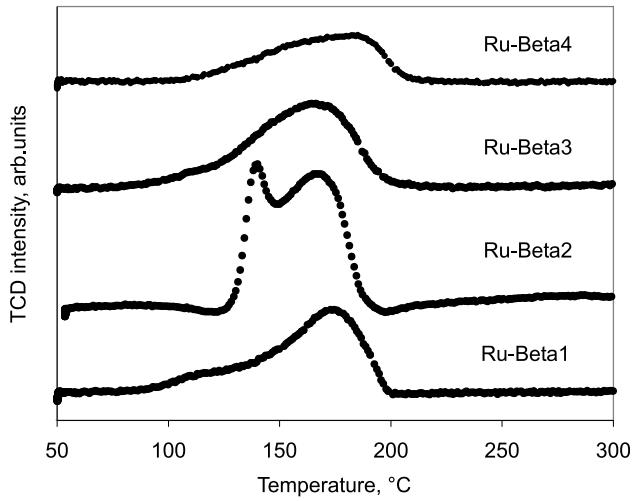

Figure 1. TPR diagrams of Ru beta zeolites.

support surface. A similar phenomenon was observed by Tway *et al.* for Y-zeolite [16]. They reported that the impregnation with $RuCl_3$ causes decrease in the surface area due to dealumination of the lattice.

The combination of TPR and XRD methods was used to understand the effect of beta zeolite acidity on the redox behaviour of ruthenium and on the crystallite size. The TPR profiles for the Ru beta zeolites are displayed in figure 1. The crystallite sizes of Ru-Beta4 as they depend on the reduction temperature are summarised in table 3. The TPR reduction temperatures, dispersions and crystallite sizes for the Ru beta catalysts are collected in table 4. All Ru beta zeolite catalysts exhibited two maxima in the TPR curve fitting. This finding is in good agreement with the results reported by Bischhof *et al.* [17] on Ru supported on MCM-41 and MCM-48 zeolites. As an example, the Ru-Beta4 catalyst showed two TPR peaks at temperatures of 145 and 175 °C (see table 4). The XRD results in table 3 show that this catalyst has two phases, RuO_2 and metallic Ru, at the low reduction temperature of 120 °C. At reduction temperature of 170 °C, however, no RuO_2 phase was observed. The Ru-Beta1, Ru-Beta3 and Ru-Beta4 catalysts have low Brönsted acidity compared with Ru-Beta2. The shapes of the TPR curves were similar and showed only one peak with shoulder, while the TPR curve of Ru-Beta2 showed two distinct peaks. The reduction maximum temperature was also shifted 5–25 °C higher in the least acidic Ru-Beta4 relative to the more acidic Ru-Beta2, Ru-Beta3 and Ru-Beta1.

Three interpretations can be suggested for the results obtained by TPR analysis. First, the TPR peaks of the Ru beta zeolites might be due to the reduction of the bulk RuO_2 formed in the calcinations. The external surface of the RuO_2 particle might first be reduced at low temperatures giving rise to the first peak or

Table 3
Crystallite sizes of Ru-Beta4 catalyst as a function of reduction temperature

Materials	Reduction temperature, °C	Beta[a], nm	RuO_2[b], nm	Ru_{met}[c], Nm	Phases identified
Beta4, calcined at 500 °C		21.5	–	–	Beta
Ru-Beta4, calcined at 500 °C		16.5	22.0	–	Beta, RuO_2
Ru-Beta4	120	13.0	19.0	8.5	Beta, RuO_2, Ru_{met}
Ru-Beta4	170	16.5	–	8.0	Beta, Ru_{met}
Ru-Beta4	250	15.0	–	11.5	Beta, Ru_{met}
Ru-Beta4	360	16.5	–	21.0	Beta, Ru_{met}
Ru-Beta4	550	16.5	–	33.0	Beta, Ru_{met}

[a]Measured at angle 22.5° 2Θ at orientation [302].
[b]Measured at angle 35.0° 2Θ at orientation [101].
[c]Measured at angle 43.9° 2Θ at orientation [101].

Table 4
Reduction temperatures 1 and 2, dispersion, particle size and crystallite size of the Ru catalysts on beta zeolite

Catalyst	TPR (1), °C	TPR(2), °C	Dispersion, %	Ru^o particle size, nm[a]	Ru^o crystallite size, nm[b]
Ru-Beta1	120	180	2.7	52	11
Ru-Beta2	140	170	1.5	94	14
Ru-Beta3	130	170	0.9	161	11
Ru-Beta4	145	175	0.4	360	12

[a]Measured by CO chemisorption.
[b]Measured by XRD.

shoulder in the curve. The maximum in the hydrogen consumption in TPR analysis would then be related to the complete reduction of bulk RuO_2. The second interpretation assumes the formation of two phases during the calcination, bulk RuO_2 and RuO_x-Z, which is probably still interacting with the zeolite support. The two hydrogen consumption maxima would then related to the reduction of these two phases. Depending on the acidity of the beta zeolite, the ratio of the bulk RuO_2 to the ruthenium interacted with zeolite varied. The amount of ruthenium interacting with zeolite would be thus increased with increasing of zeolite acidity. Therefore, less or more RuO_2 could be formed during the calcination of the beta zeolites with different acidity. This interpretation is supported by the different shapes of the TPR curves depending on the Brönsted acidity of the zeolite. A third interpretation of the two maxima could be heterogeneity of the bulk ruthenium oxide.

As seen by XRD (table 3) increase in the temperature above 170 °C causes an increase in crystallite size of ruthenium. The further increase of temperature causes crystallisation and grain growth. Migration is evidently proceeding from small crystallites to larger crystallites.

The correlation between the particle size and the acidity shown in figure 2 describes the effect of the acidity on the particle size of metallic ruthenium. Ruthenium particles were smallest for ruthenium catalysts on beta zeolite with high acidity and largest for beta zeolite with low acidity.

The dispersions of metallic ruthenium on beta zeolites were low, between 0.4 and 2.7% (table 4). In agreement with the literature our catalysts, which were prepared on beta zeolite by impregnation technique using $RuCl_3$ as precursor, exhibited low dispersion and large ruthenium particles. The precursor used, the method of catalyst preparation and treatment have been shown to have a clear effect on the ruthenium dispersion [15,17,18]. Thus, the exposure of catalyst to oxygen results in the quantitative oxidation of ruthenium to RuO_2 and subsequent reduction in hydrogen causes progressive migration of the ruthenium to form large metal particles. The particle sizes of ruthenium were larger than the crystallite sizes. This indicates that the ruthenium particles have numerous defects.

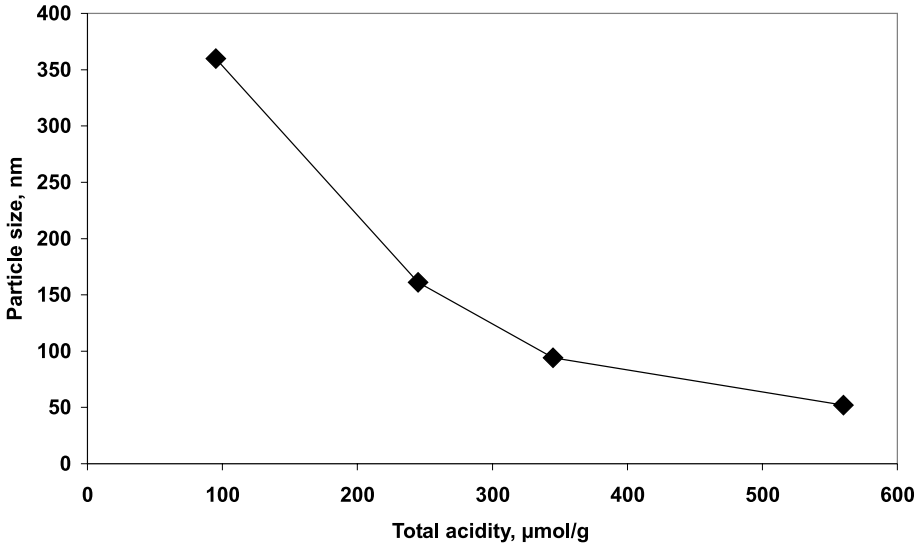

Figure 2. Total acidity of catalysts versus particle sizes of ruthenium reduced at 250 °C.

3.2. Catalytic properties

3.2.1. Activity of the catalysts and reactivity of surface ruthenium atoms

The conversions of the catalysts and the TOF values are summarised in table 5. The total acidity influenced the particle sizes (figure 2), which clearly then affected the activity of the catalysts in cinnamaldehyde hydrogenation. The highest conversions of cinnamaldehyde were obtained with Ru-Beta2, which possessed highest Brönsted acidity. The second highest conversion was with Ru-Beta1, which had the highest number of acid sites, the highest dispersion and the smallest particle size. Low conversions were obtained with the Ru-Beta3 and Ru-Beta4 catalysts, which had a smaller number of acid sites and large ruthenium particle size.

The TOF_h value for hydrogenation was highest with the catalyst Ru-Beta4, which had the largest ruthenium particles. This observation agrees with our earlier work with palladium and ruthenium on silica and alumina supports [21]. The TOF_a value for acetal formation was highest with the catalyst Ru-Beta2 which had the largest number of Brönsted acid sites.

The Brönsted acidity of the catalysts is plotted versus the ratio of acid catalysed to hydrogenated products in figure 3. The activities of the catalysts towards the products formed on acid sites increased with the Brönsted acidity.

3.2.2. Selectivity of the catalysts

The reaction pathway of cinnamaldehyde hydrogenation was described in our previous paper [21]. In general, hydrogenation of cinnamaldehyde leads to hydrogenated, dehydrated and acid-catalysed products. Hydrocinnamaldehyde was formed with all the Ru beta zeolite catalysts and no other hydrogenated products were observed. Cinnamaldehyde acetal and hydrocinnamaldehyde acetal were formed as acid-catalysed products. The reaction scheme is presented in figure 4.

The selectivities of ruthenium beta zeolites as a function of particle size of ruthenium at conversion of 5% are presented in figure 5. It shows that the formation of hydrocinnamaldehyde was dependent on the particle size and acidity of the catalysts. The selectivity to hydrocinnamaldehyde increased with the particle size and decrease in the number of acid sites.

Table 5
Conversions and TOF values of the catalysts

Catalysts	Total conversion, % (4 h)	*TOF_h, 1/s Ru^0 site	**TOF_a, 1/s acid site	Ratio of acid-catalysed to hydrogenated products, wt%/wt%
Ru-Beta1	16	0.11	0.02	1.2
Ru-Beta2	25	0.10	0.12	5.1
Ru-Beta3	8	0.12	0.01	1.4
Ru-Beta4	12	1.7	0.03	0.5

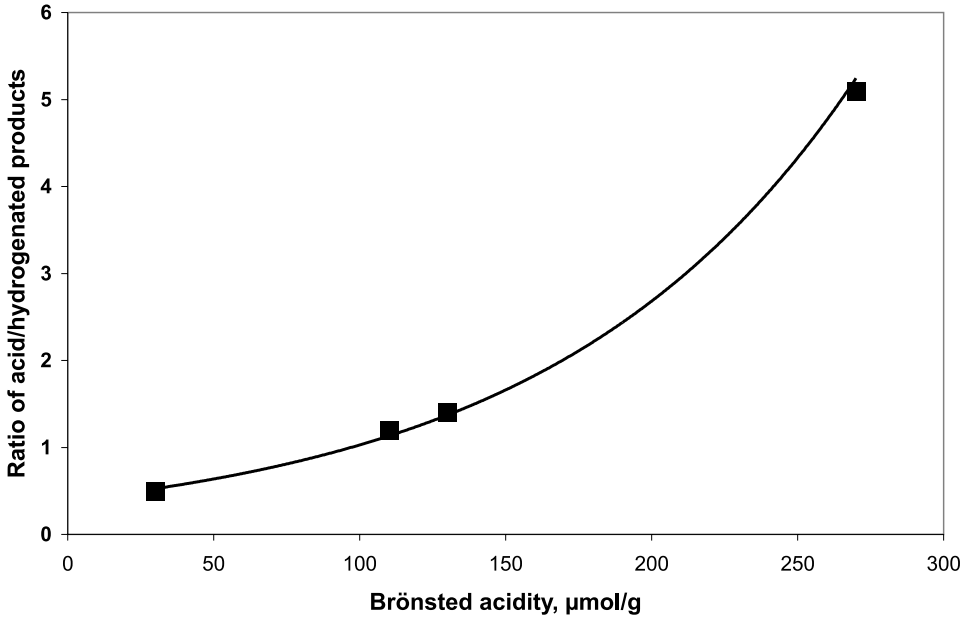

Figure 3. Brönsted acidity versus the ratio of acid-catalysed products to hydrogenated products.

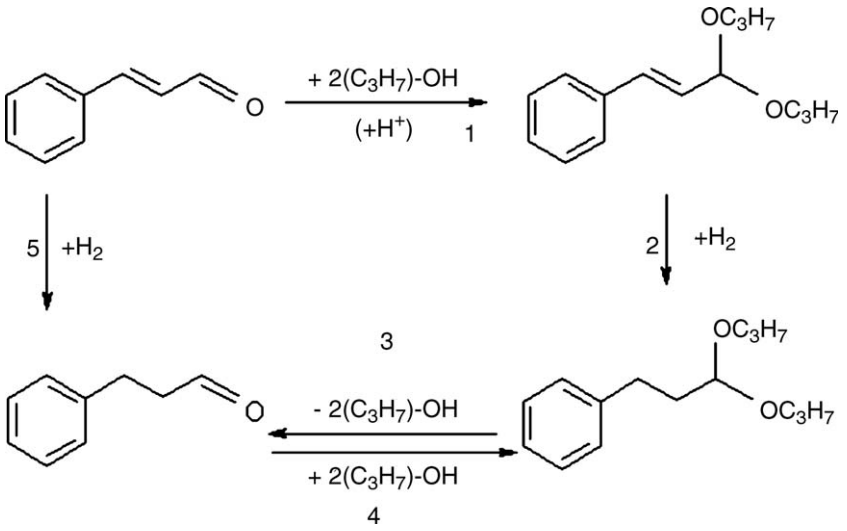

Figure 4. Reaction pathway of the products formed with the use of Ru beta zeolite catalysts in cinnamaldehyde hydrogenation.

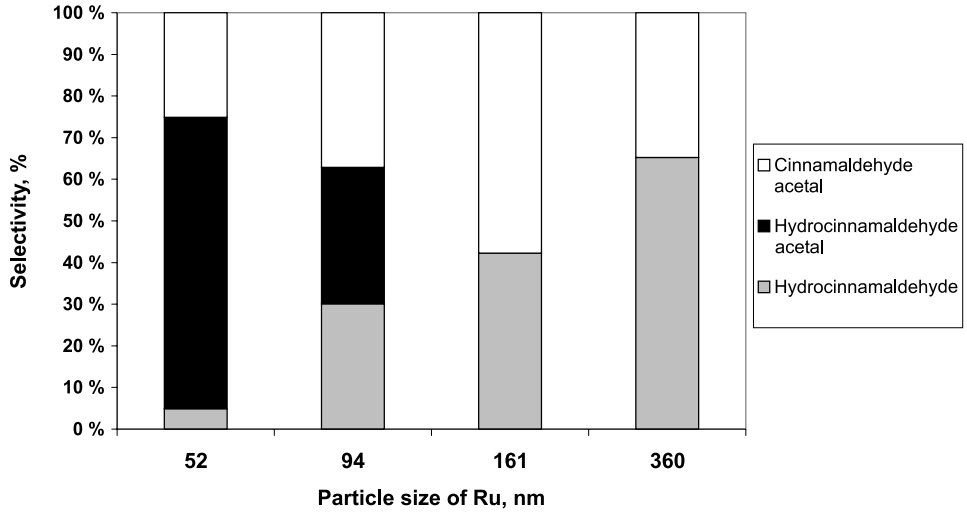

Figure 5. Selectivity of different Ru beta zeolites versus particle sizes.

The high acidity of the Ru-Beta1 and Ru-Beta2 catalysts leads to initial formation of cinnamaldehyde acetal through reaction between cinnamaldehyde molecule and the solvent isopropanol, with the result that the C=O group of cinnamaldehyde is protected. This protection prevents the adsorption of C=O and the formation of cinnamyl alcohol. The cinnamaldehyde acetal is further hydrogenated to hydrocinnamaldehyde acetal, which readily undergoes hydrogenolysis to hydrocinnamaldehyde. This interpretation is in good agreement with that of Millman and smith. [31], who suggested that with Pd on η-alumina catalysts the hydrocinnamaldehyde and its acetal were formed from cinnamaldehyde acetal rather than cinnamaldehyde. The reaction pathway also agrees with Billman *et al.* [32], who describe a method to prepare hydrocinnamaldehyde from cinnamaldehyde through its acetal by protection of the C=O group of cinnamaldehyde.

Hydrocinnamaldehyde was still not observed after 2 h hydrogenation, whereas the hydrocinnamaldehyde acetal was formed, but it was present after 4 h with a corresponding decrease in the amount of hydrocinnamaldehyde acetal. This finding provides additional evidence of the proposed reaction route. However, the formation of hydrocinnamaldehyde acetal was only observed with the Ru-Beta1 and Ru-Beta2 catalysts, which have the greatest number of acid sites and the smallest ruthenium particles.

On Ru-Beta3 and Ru-Beta4, only hydrocinnamaldehyde and cinnamaldehyde acetal were observed. The amount of the acetal formed with Ru-Beta3 was greater than that formed with Ru-Beta4 because of the higher acidity of the Ru-Beta3 compared with Ru-Beta4. The poor dispersion and the large particle sizes of ruthenium in Ru-Beta3 and Ru-Beta4 might explain why no hydrocinnamaldehyde acetal was observed. Namely, a

steric effect arises from the aromatic ring exist at the head of the molecule and the two isopropyl groups in the tail prevent the planar adsorbing of cinnamaldehyde acetal molecule parallel to a flat metal surface. As a result, the C=C bond can not approach the surface closely enough to be hydrogenated.

Despite the large particle size of the catalysts, neither cinnamyl alcohol or its hydrogenated product 3-phenyl-1-propanol was formed. Evidently the large ruthenium metal particle supported on beta zeolite catalyst activates only the C=C bond of the cinnamaldehyde molecule. This observation is in contrast to that reported by Gallezot and Richard. [11] for ruthenium supported on carbon and in good agreement with our previous results [21] for ruthenium supported on alumina and silica.

4. Conclusions

The addition of ruthenium to beta zeolite by wet impregnation of $RuCl_3$ decreased the crystallite size of the zeolite. The acidity of the beta zeolite affected the reduction behaviour of ruthenium, and it affected the particle size, which increased as the acidity decreased. The acidity also influenced the activity and selectivity of the catalysts. The catalyst with highest Brönsted acidity yielded the highest conversion of cinnamaldehyde. Generally, both cinnamyl alcohol and hydrocinnamaldehyde are formed in cinnamaldehyde hydrogenation with the Ru catalysts, and with large Ru particles the formation of cinnamyl alcohol should be predominant. With our Ru beta catalysts, only hydrocinnamaldehyde, cinnamaldehyde acetal and hydrocinnamaldehyde acetal were formed. The lack of cinnamyl alcohol formation can be explained by the protection of the C=O group of cinnamaldehyde by acetal formation during the hydrogenation, and the Ru beta zeolite catalysts were only selective to C=C bond hydrogenation.

Acknowledgments

We wish to thank Dr. A. Root, H. Leuku and R. Vuorenmaa (Fortum Oil and Gas) for carrying out the NMR, XRD and BET measurements. Dr. K. Ahonen improved the English language of the manuscript. Support was provided by the Academy of Finland and Fortum Foundation.

References

[1] M.D. Cisneros and J.H. Lunsford, J. Catal. 141 (1993) 191.
[2] D. Ballivet-Tkatchenko, N. Chau, H. Mozzanega, M. Roux and I. Tkatchenko, ACS Symposium Series 152 (1981) 187.
[3] I.H. Cho, S.J. Cho, S.B. Park and R. Ryoo, J. Catal. 153 (1995) 232.
[4] T.G. Harvey and K.C. Pratt, Appl. Catal. A: Gen. 146 (1996) 317.
[5] S. Kawi, S. Liu and S.-C., Shen, Catal. Today 68 (2001) 237.
[6] J.Y. Bae and W.Y. Lee, Stud. Surf. Sci. Catal. 125 (1999) 611.
[7] R.K. Graselli, R.M. Lago, R.F. Socha and J.G. Tsikoyiannis, US Patent 5 37 4410.
[8] K. Bauer and D. Garbe, Common Fragrance and Flavor Materials (VCH, Weinheim,1985).
[9] K. Bauer and D. Garbe, in: *Ullman Encyclopedia*, Vol. All (VCH, New York, 1988) p. 141.
[10] K. Weissermel and HJ. Arpe, *Industrial Organic Chemistry* (Verlage Chemie, Weinheim, 1978).
[11] P. Gallezot and D. Richard, Catal. Rev.-Eng. 40 (1998) 81.
[12] D. Blackmond, R. Oukaci, B. Blanc and P. Gallezot, J. Catal. 131 (1991) 401.
[13] G. Li, T. Li, Y. Xu, S. Wong and X. Guo, Stud. Surf. Sci. Catal. 105 (1997) 1203.
[14] S. Galvagno and G. Capannelli, J. Mol. Catal. 64 (1991) 237.
[15] V. Parvulescu, S. Coman, P. Palade, D. Macovei, C. Teodorescu, G. Filoti, R. Molina, G. Poncelet and F. Wagner, Appl. Surf. Sci. 141 (1999) 164.
[16] C. Tway, S. Bonafede, A. Ghazi, C. Reed, R. DeAngelis and T. Apple, ACS Symp. Series 517 (1993) 372.
[17] C. Bischof and M. Hartmann, Proc. Int. Zeolite Conf. 2 (1999) 809.
[18] V.I. Parvulescu, V. Parvulescu, S. Kaliaguine, U. Endruschat, B. Tesche and H. Bönneman, in: *Catalysis of Organic Reaction*, ed. M.E. Ford (Wiley-Interscience, New York, Basel, 1982) p. 301.
[19] S. Galvagno, A. Donato, G. Neri and R. Pietropaolo, J. Mol. Catal. 64 (1991) 237.
[20] S. Galvagno, C. Milone, A. Donato, G. Neri and R. Pietropaolo, Catal. Lett. 18 (1993) 349.
[21] M. Lashdaf, A.O.I. Krause, M. Lindblad, M. Tiitta and T. Venäläinen, Appl. Catal. A: Gen. 241 (2003) 65.
[22] *Handbook of Heterogeneous Catalysis*, Vol. 1, eds. G. Ertl, H. Knözinger and J. Weitkamp (VCH Wiley Company, 1997) p. 324.
[23] A. Corma, Chem. Rev. 95 (1995) 559.
[24] P.J. Kunkeler, D. Moeskops and H. van Bekkum, Micropor. Mater. 11 (1997) 313.
[25] G. Leafanti, M. Padovan, G. Tozzola and B. Venturalli, Catal. Today 41 (1998) 207.
[26] Handbook of Heterogeneous Catalysis, Vol. 2, eds. G. Ertl, H. Knözinger and J. Weitkamp (VCH Wiley Company, 1997) p. 447.
[27] *X-Ray Diffraction Procedures*, eds. H.P. Klug and L.E. Alexander 2.nd ed. (John Wiley & Sons, 1974) p. 687.
[28] P. Rylander and N. Himelstein, Engelhard Ind. Tech. Bull. 4 (1964) 131.
[29] M. Lashdaf, A. Hase, E. Kauppinen, A.O. Krause, Catal. Lett. 52 (1998) 199.
[30] S. Galvagno and G. Capannelli, J. Mol. Catal. 64 (1991) 237.
[31] W.S. Millman and G.V. Smith, in: *Catalysis in Organic Synthesis* (Academic Press, New York, 1980) p. 33.
[32] J.H. Billman, J.I. Stiles and J. Tonnis, Synth. Commun. 1 (1971) 127.